

From nanorod of palygorskite to nanosheet of smectite *via* one-step hydrothermal process

Wenbo Wang^{a,c}, Zhifang Zhang^{a,b}, Guangyan Tian^{a,b}, Aiqin Wang^{a,c*}

^aCenter of Eco-material and Green Chemistry, Lanzhou Institute of Chemical Physics, Chinese Academy of Sciences, Lanzhou 730000, P.R. China

^bUniversity of the Chinese Academy of Sciences, Beijing 100049, P.R. China

^cR&D Center of Xuyi Palygorskite Applied Technology, Lanzhou Institute of Chemical Physics, Chinese Academy of Sciences, Xuyi 211700, P.R. China

Experimental section

Hydrothermal process of PAL

The pre-treated PAL powders were uniformly dispersed in 60 mL deionized water under magnetic stirring, and then the resultant suspension was transferred into a 100-mL Teflon Tank, sealed and then reacted at different temperature for 48 h. To study the effect of ball milling time, the PAL was grinded for 0h, 2h, 4h, 8h and used for hydrothermal reaction. To study the effect of solid/liquid ratio, the solid/liquid ratio of 1:300, 1:200 and 1:120 was selected. To study the effect of reaction temperature, the 140°C, 160°C and 180°C was selected. To study the effect of pH values, the initial pH values of the dispersion for hydrothermal reaction were adjusted to pHs 4, 5, 6, 7, 8, 9, 10, 11 using HCl or NaOH solution. To study the effect of CaCO₃, the CaCO₃ powder was added before hydrothermal reaction. The resultant solid product was separated by centrifugation at 5000 r/min, fully washed for 10 times, and then dried under vacuum at 60 °C to a constant mass. The dry product was ground and passed through a 200-mesh sieve for further use.

Results and discussion

Effect of grinding time

The moderate grinding is essential to the transformation of PAL crystal. The previous work [1] has proved that the moderate mechanical treatment may promote the

dissolution of the metal ions in the crystal backbone of PAL. In order to explore the effect of grinding on the transformation behavior, we compared the un-grinding sample and the grinded sample for different time, and studied the change of crystal structure of the PAL with and without grinding after hydrothermal process.

The SEM micrographs of the RPAL before and after hydrothermal treatment are shown in Fig. S1. The un-grinded PAL shows rod-like morphology after hydrothermal treatment. After hydrothermal reaction, the rod-like morphology has no obvious change, and only some particles or purities were reduced. But, the situation is difficult for grinded PAL. After grinded RPAL for 1h, the number of rod-like crystals were obvious reduced and the number of sheet-like crystal increased, and many rod-sheet phase was observed. With prolonging the grinding time to 6h, the number of rods was further decreased, and almost no rods can be observed for the hydrothermal sample grinding for 6h, and only the sheet-like structure appeared. It indicates that the mechanical grinding is beneficial to the evolution of PAL to other crystal phase. Fig. S2 give a more clear evidence for the transformation. It is obvious that the (110) peak of PAL at about $2\theta=8.43^\circ$ obviously weakened after hydrothermal treatment of the PAL grinded for different time. For PAL grinded for 6h, the (110) peak almost disappeared, and the new peak at $2\theta=6.05^\circ$ appeared, which confirms that grinding for 6h is favorable to the transformation of PAL into smectite. The grinding time of 6h is enough to the transformation of PAL under hydrothermal condition.

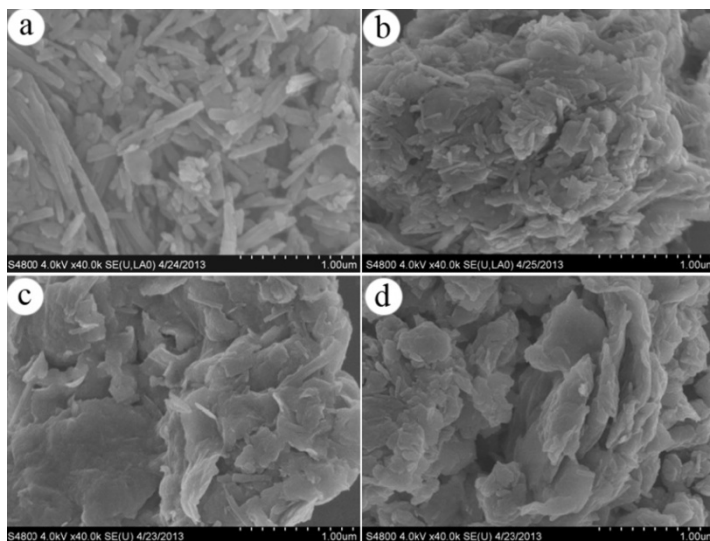


Fig. S1. SEM micrographs of hydrothermally treated PAL: (a) un-grinded PAL; (b)

grinded PAL for 1h, (c) grinded PAL for 2h, (d) grinded PAL for 6h.

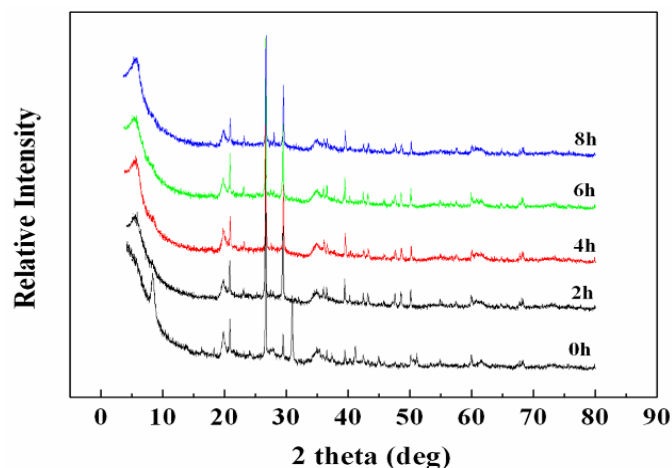


Fig. S2. XRD patterns of the hydrothermally treated PAL grinded from different time.

Effect of reaction temperature

The effect of reaction temperature was studied to explore the more moderate temperature for the transformation process. The XRD patterns of PAL treated at 140°C, 160°C and 180°C are shown in Fig. S3. As can be seen, the (110) characteristic peak of PAL appeared at about $2\theta = 8.4^\circ$. After treated at 140°C, these peaks are slightly decreased, indicating that the crystal structure has not been transformed at this temperature. When the temperature was increased to 180°C, the peak almost disappeared, and new peak at $2\theta = 6.05^\circ$ (001 peak of smectite) was observed, which confirms the transformation of PAL crystal to smectite. The temperature of 180°C is suitable for the transformation process of PAL.

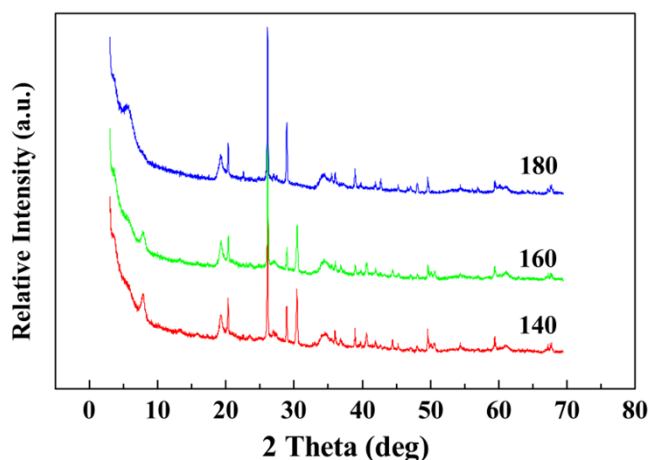


Fig. S3. XRD patterns of PAL treated at (a) 140°C, (b) 160°C and (c) 180°C.

Effect of pH values

Fig. S4 shows the SEM images of hydrothermally treated PAL at different pH values. The results are consistent with the FTIR analysis. It was found that the PAL rods are still excised after hydrothermal treatment at pH 5. With increasing the pH values, the rod was gradually reduced, and the increase of pH is favorable to the transformation of PAL rods into the sheet-like smectite.

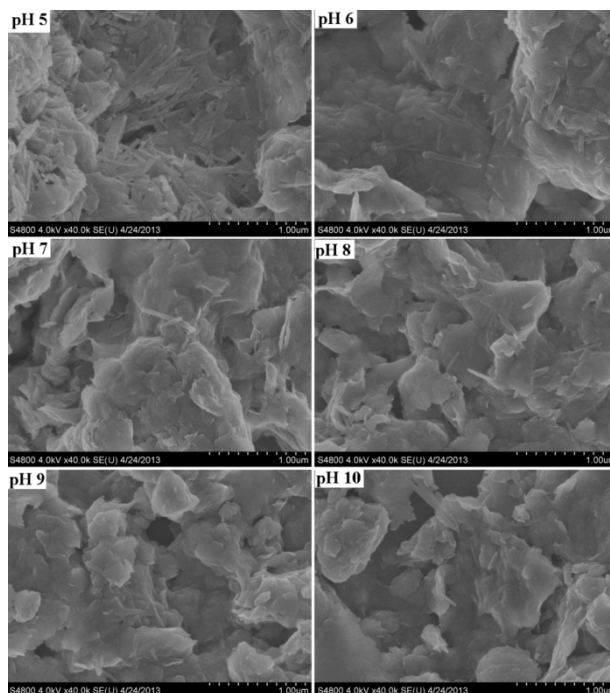


Fig. S4. SEM micrographs of raw PAL after hydrothermal treatment at different pH values.

Fig. S5 shows the XRD patterns of hydrothermally treated PAL at different pH values. It was found that the 110 characteristic peak of PAL was weakened after hydrothermal treatment at pH 4 and 5. With increasing the pH values, the 110 diffraction peak disappears, and the new peak at $2\theta=6.05^\circ$ appeared. This indicates that the $\text{pH}>6$ is necessary for the transformation of PAL crystal, and the higher pH values are beneficial to the transformation process.

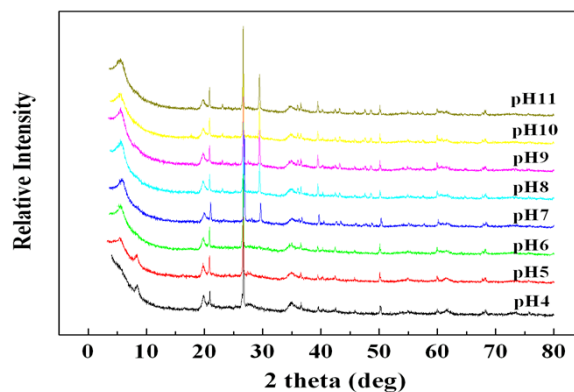


Fig. S5 XRD patterns of RPAL treated at different pH values

Effect of acidification treatment of PAL on transformation

Fig. S6 shows the SEM images of hydrothermally treated APAL (after pretreated by acidification) at different pH values. It was observed that the rod crystals could be obviously observed in each sample. Even at pH 10, much rod crystals could be observed in the hydrothermally treated product. This is consistent with the XRD results of APAL after treated for different time (Fig. S7), and confirms that the removal of carbonates is adverse to the transformation of PAL crystals.

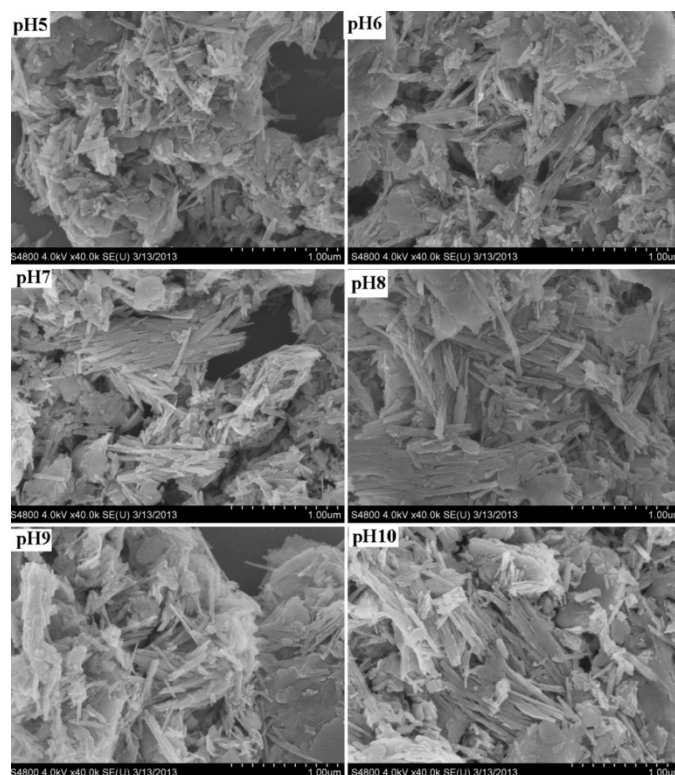


Fig. S6. SEM micrographs of acidified PAL after hydrothermal treatment at different pH values.

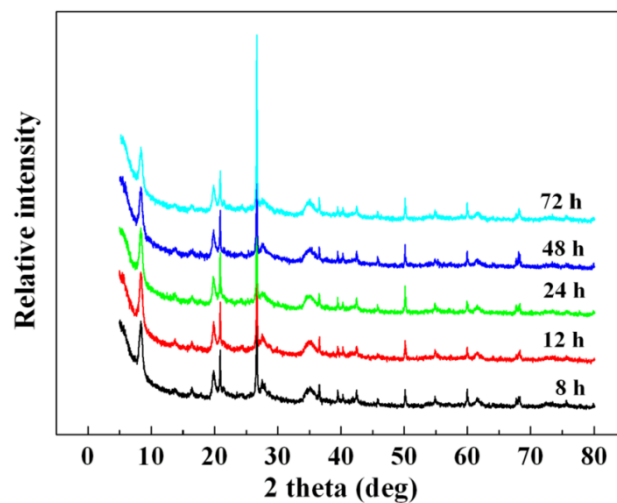


Fig. S7. XRD patterns of acidified PAL (APAL) after hydrothermal treatment for different time.

Effect of adding CaCO_3

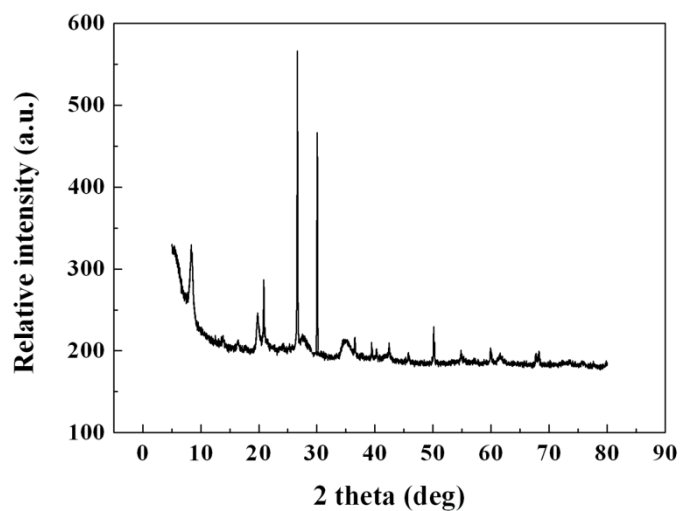


Fig. S8. XRD patterns of acidified PAL after hydrothermal treatment by adding different amount of CaCO_3 .

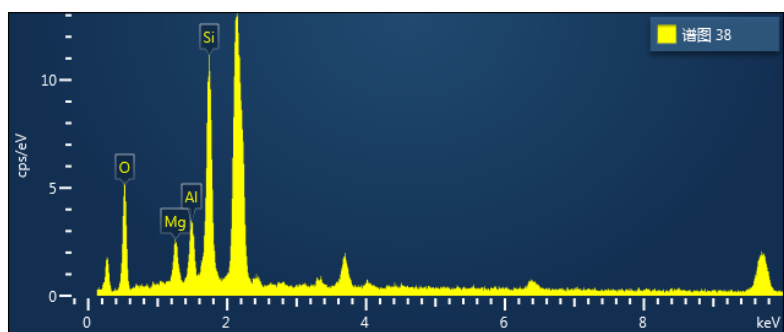


Fig. S9 EDX spectrogram of the raw palygorskite

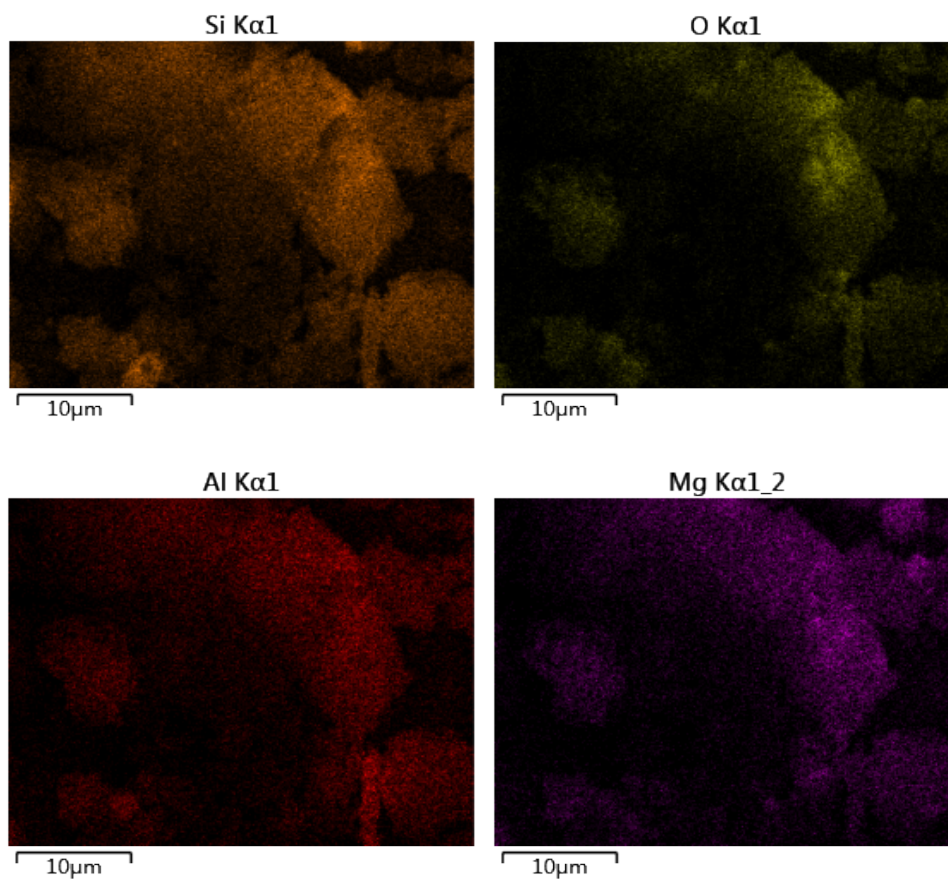


Fig. S10 Elemental mapping of the raw PAL

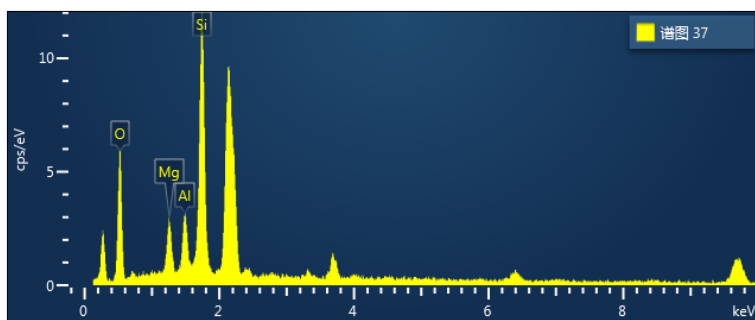


Fig. S11 EDX spectrogram of RPAL-48h (hydrothermal treatment of RPAL for 48h)

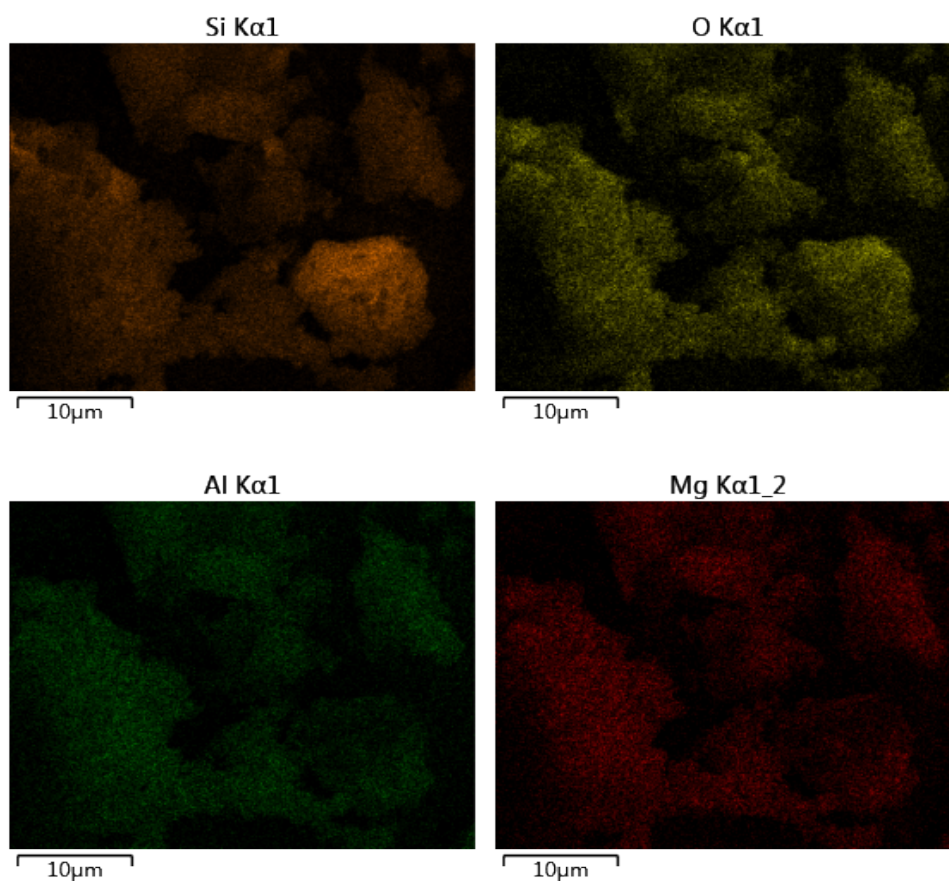


Fig. S12 Elemental mapping of RPAL-48h (hydrothermal treatment of RPAL for 48h)

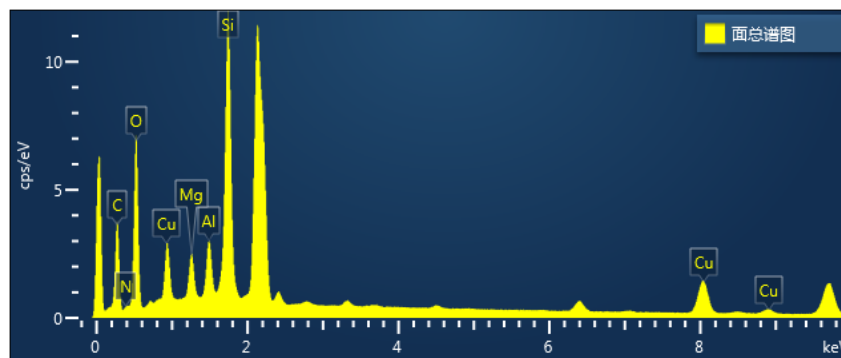


Fig. S13 EDS spectrogram of RPAL-48h (hydrothermal treatment of RPAL for 48h) after adsorption of Cu(II)

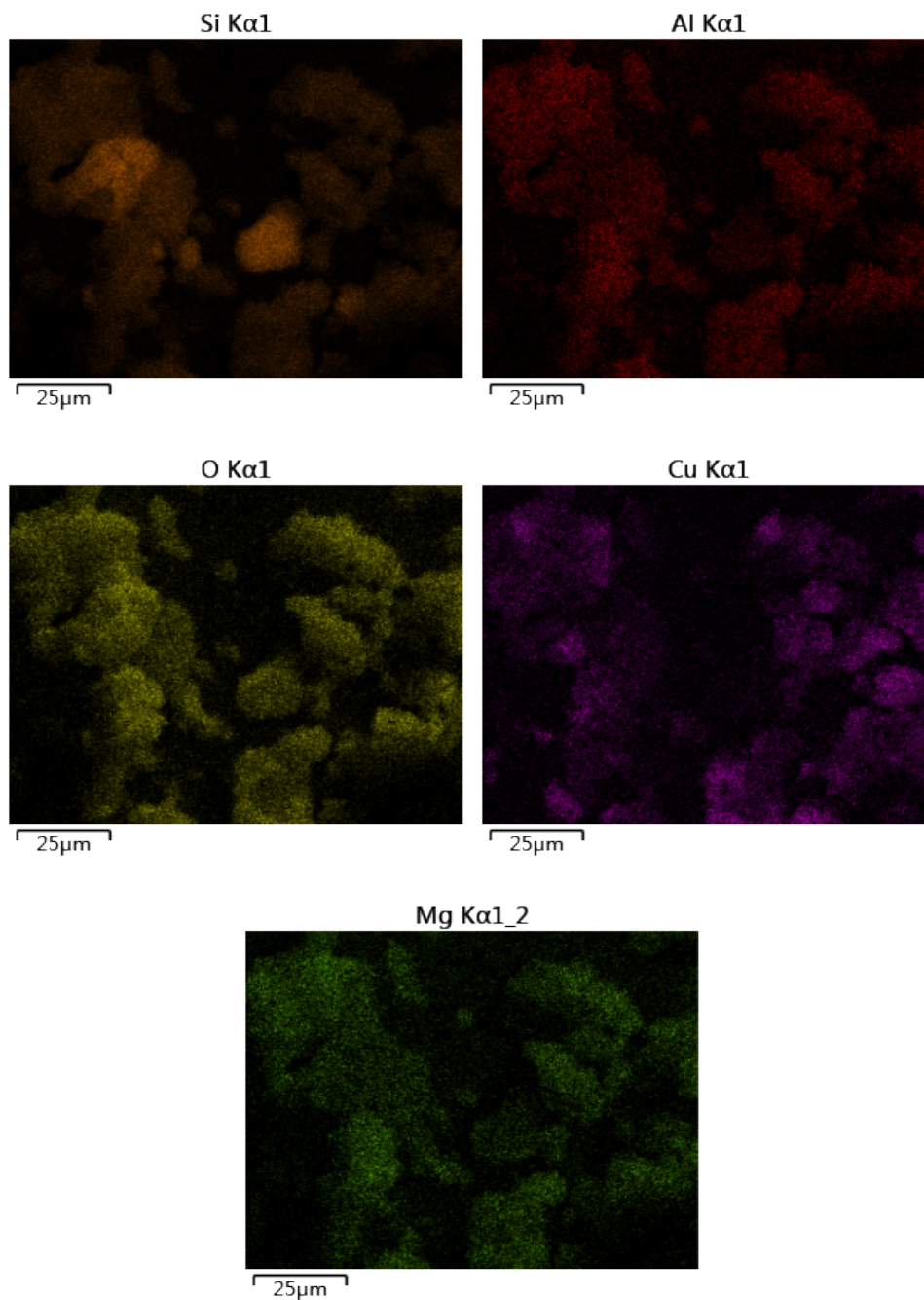


Fig. S14 Elemental mapping of RPAL-48h (hydrothermal treatment of RPAL for 48h) after adsorption Cu(II)

XRF analysis

The change of chemical composition of PAL before and after hydrothermal reaction is listed in [Table S1](#). As can be seen, the chemical composition of PAL has minor change after hydrothermal reaction. The content of Al_2O_3 was initially increased and then decreased, and the MgO content was gradually increased with prolonging the

reaction time, but the increasing tendency is not obvious. This confirms that the chemical composition has no change despite that the crystal structure was changed as confirmed by XRD, SEM and TEM. The hydrothermal process only changed the combination style of elements and fine crystal structure, instead of the intrinsic chemical composition. That is to say, a re-organization of each unit process was occurred. As known, palygorskite is enriched in Mg and smectite is slightly enriched in Al. The similarity in chemical composition before and after transformation indicating that the formed smectite is a Mg-rich mineral. The Si/Mg and Si/Al ratio was decreased after hydrothermal reaction.

Table S1. XRF chemical composition (%) of the PAL before and after hydrothermal reaction

	Al ₂ O ₃	MgO	SiO ₂	K ₂ O	Limestone	Fe ₂ O ₃	Si/Mg	Si/Al
RPAL	9.975	6.735	49.369	1.525	22.714	8.315	4.887	4.207
RPAL-2h	10.858	6.760	49.124	1.535	21.571	8.027	4.845	3.846
RPAL-4h	11.081	6.997	49.203	1.560	20.839	8.086	4.688	3.774
RPAL-8h	11.067	7.164	48.409	1.570	20.876	8.362	4.505	3.718
RPAL-24h	11.03	7.238	47.728	1.473	21.706	8.006	4.396	3.678
RPAL-48h	10.98	7.396	47.124	1.501	22.246	8.833	4.248	3.648

BET specific surface area analysis

Table S2. Microstructural parameters of PAL before and after hydrothermal treatment

Samples	S_{BET} (m ² /g)	S_{ext} (m ² /g)	S_{micro} (m ² /g)	V_{micro} (cm ³ /g)	PZ (nm)	PV (cm ³ /g)
RPAL	123.83	83.29	40.54	0.0182	7.2265	0.2237

RPAL-2h	117.81	88.55	29.26	0.0129	7.6616	0.2257
RPAL-4h	116.15	87.97	28.18	0.0125	7.8999	0.2294
RPAL-8h	105.35	83.56	21.79	0.0094	7.8644	0.2071
RPAL-24h	98.61	78.02	20.59	0.0088	6.4107	0.1581
RPAL-48h	94.06	78.85	15.21	0.0062	5.8202	0.1369
APAL-48h	104.57	75.18	29.39	0.0131	10.9089	0.2852

Reference list

[1] Yang, H., Tang, A., Ouyang, J., Li, M., & Mann, S. (2010). From natural attapulgite to mesoporous materials: methodology, characterization and structural evolution. *The Journal of Physical Chemistry B*, 114(7), 2390-2398.